Analysis of the NCal data collected during O3B

B. Mours, T. Pradier (IPHC)

March 10, 2020 *

VIR-0268A-20

The authors would like to thanks B. Lieunard, L. Journet, G. Deleglise and S. Petit from LAPP for the design, assembly, metrology and control system of the NCal-200, as well as E. Dangelser from IPHC for the modification of the NCal support.

Abstract

This note described the tests made with the NCal during the O3B data taking period, up to end of February 2020.

Contents

*Two typos fixed page 9 and 15 on March 14

1 Introduction: evolution of the NCal system during O3B

A few tests have been made during O3B with the so called NCal-200 (build at LAPP). The first tests were made with just one NCal-200 hanging from a vertical support on the south side of the north end tower. There were some disagreements, at a few percent level, between the expected and recovered signals.

The NCal signal is known to be very sensitive to the mirror-NCal distance. This is why, during the October 2019 test, two positions were used to extract this mirror-NCal distance, that turned out to be off by more than a centimeter compared to the expected value, a too large offset given our knowledge of the mirror position.

More data were remotely collected on December 18. The confirmed the few percent overall disagreement, although frequency dependence of the injected versus recovered signal seems to reproduce the shape observed with the PCal or electromagnetic actuators.

On January 21, A second NCal-200 was installed on the north side (see left picture of figure 1) and further data were collected with the south NCal being at two different locations. This test highlighted that the hanging system of the NCal was not providing a reproducible location of the NCal system. Despite the accurate measurements of the support points, the two rods supporting the NCal could have their relative length changing a bit leading to offset of several mm at the NCal level, making impossible the accurate knowledge of the NCal position, even between two NCal positions.

To solve this issue, a new layout was designed with both NCal-200 suspended from a single plate, hanging from the support beam, see right picture of figure 1. With this new layout, the distance between the two NCal is well defined. Thanks also to the large distance between the hanging rods, the NCal position itself is now better related to the one of the top supporting beam.

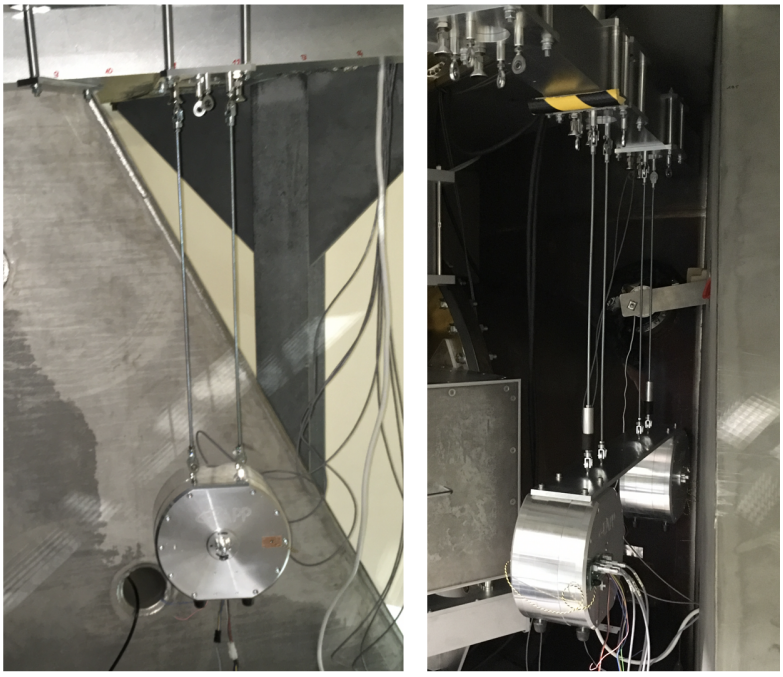

Figure 1: The left picture shows one NCal-200 suspended on the north side of the north end tower. The right picture shows two NCal-200 suspended from the same support plate on the south side of the north end tower

2 Predicting the signal induced by a vertical NCal

In this section, we derive the effect of a simple rotor on the position of one of the interferometer mirrors. First we use a very simple point-like model of a device aligned on the beam axis to show the basic characteristics of the signal to be observed in the $h(t)$ gravitational wave strain. Then we consider an off-axis device and a more realistic extended rotor. These computation are slightly different from the one in the 2018 NCal paper (`https://arxiv.org/pdf/1806.06572.pdf`), which was focusing on an horizontal rotor, instead of a vertical one as it is the case for the NCal-200.

2.1 Two point-like masses aligned on the beam axis

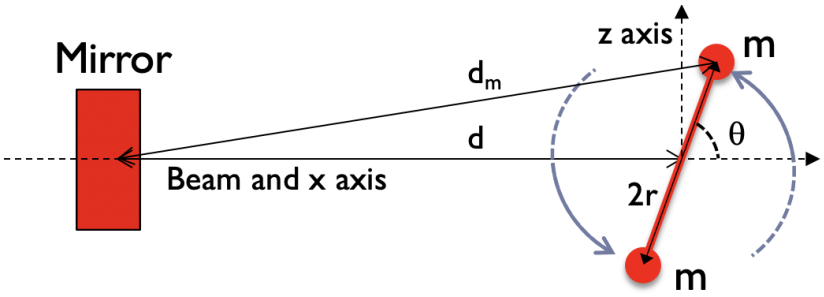

Figure 2: Simple rotor made of two masses

The simplest possible version of an NCal is a system of two point-like masses m separated by a distance $2r$, on a rotor rotating at frequency f, located at a distance d from the mirror of mass M (see figure 2). The mirror is also assumed to be point-like.

For this initial computation, we assume that the rotor center is aligned on the beam axis that is our x axis ($\Phi = 0$). The coordinates of one mass m relative to the mirror position are then $(x = d + r\cos\theta); (y = r\sin\theta)$. Therefore the distance between the mirror and one mass is:

$$d_m = d\sqrt{(1 + 2\epsilon\cos\theta + \epsilon^2)} \text{ with } \epsilon = r/d \tag{1}$$

The gravitational force applied by the first mass on the mirror is:

$$F_1 = \frac{GMm}{d_m^2} \tag{2}$$

Its projection along the beam axis is:

$$F_{1x} = \frac{GMm}{d^2}T \tag{3}$$

With

$$T = (1 + \epsilon\cos\theta)(1 + 2\epsilon\cos\theta + \epsilon^2)^{-3/2} \tag{4}$$

Since the fourth order Taylor development of the -3/2 power is :

$$(1 + x)^{-3/2} = 1 - \tfrac{3}{2}x + \tfrac{15}{8}x^2 - \tfrac{35}{16}x^3 + \tfrac{315}{128}x^4 + ... \tag{5}$$

With

$$x = 2\epsilon\cos\theta + \epsilon^2 \tag{6}$$

And therefore (ignoring ϵ^5 and higher order terms)

$$x^2 = 4\epsilon^2 \cos^2\theta + 4\epsilon^3 \cos\theta + \epsilon^4 \tag{7}$$
$$x^3 = 8\epsilon^3 \cos^3\theta + 12\epsilon^4 \cos^2\theta \tag{8}$$
$$x^4 = 16\epsilon^4 \cos^4\theta \tag{9}$$

We have:

$$\begin{aligned}(1+x)^{-3/2} = 1 &- \tfrac{3}{2}(2\epsilon\cos\theta + \epsilon^2) \\ &+ \tfrac{15}{8}(4\epsilon^2\cos^2\theta + 4\epsilon^3\cos\theta + \epsilon^4) \\ &- \tfrac{35}{16}(8\epsilon^3\cos^3\theta + 12\epsilon^4\cos^2\theta) \\ &+ \tfrac{315}{128}(16\epsilon^4\cos^4\theta) + ...\end{aligned} \tag{10}$$

Or:

$$\begin{aligned}(1+x)^{-3/2} = 1 &- \tfrac{3}{2}\epsilon^2 + \tfrac{15}{8}\epsilon^4 \\ &+ (-3 + \tfrac{15}{2}\epsilon^2)\epsilon\cos\theta \\ &+ (\tfrac{15}{2} - \tfrac{105}{4}\epsilon^2)\epsilon^2\cos^2\theta \\ &- \tfrac{35}{2}\epsilon^3\cos^3\theta \\ &+ \tfrac{315}{8}\epsilon^4\cos^4\theta + ...\end{aligned} \tag{11}$$

Inserting that result in the definition of T we get:

$$\begin{aligned}T = (1 &- \tfrac{3}{2}\epsilon^2 + \tfrac{15}{8}\epsilon^4) \\ &+ (-2 + 6\epsilon^2)\epsilon\cos\theta \\ &+ (\tfrac{9}{2} - \tfrac{75}{4})\epsilon^2)\epsilon^2\cos^2\theta \\ &- 10\epsilon^3\cos^3\theta \\ &+ \tfrac{175}{8}\epsilon^4\cos^4\theta + ...\end{aligned} \tag{12}$$

Since the power of $\cos\theta$ are:

$$\begin{aligned}\cos\theta^2 &= 1 + \cos 2\theta \\ \cos\theta^3 &= (\cos 3\theta + 3\cos\theta)/4 \\ \cos\theta^4 &= (3 + 4\cos 2\theta + \cos 4\theta)/8\end{aligned} \tag{13}$$

We have:

$$T = C_0 + C_1\cos\theta + C_2\cos 2\theta + C_3\cos 3\theta + C_4\cos 4\theta + ... \tag{14}$$

With:

$$\begin{aligned}C_0 &= 1 + \tfrac{3}{4}\epsilon^2 + \tfrac{45}{64}\epsilon^4 \\ C_1 &= -2\epsilon - \tfrac{6}{4}\epsilon^3 \\ C_2 &= \tfrac{9}{4}\epsilon^2 + \tfrac{25}{16}\epsilon^4 \\ C_3 &= -\tfrac{10}{4}\epsilon^3 \\ C_4 &= \tfrac{175}{64}\epsilon^4\end{aligned} \tag{15}$$

If the second mass is on the other side of the rotor (θ replaced by $\theta + \pi$), then, the odd terms cancel out. The total force has therefore just a modulation at two and four times the rotor rotation frequency (f_{rotor}). Of course, there is also very small higher order harmonics but they are neglected in this computation.

If this frequency is well above the proper frequency of the mirror suspension (about 0.6 Hz), the amplitude of the mirror motion at two times the rotation frequency (f_{2rotor}) is:

$$\begin{aligned} a(f_{2rotor}) &= \frac{2C_2Gm}{4\pi^2 f_{2rotor}^2 d^2} \\ &= A_2\left(1+\frac{25}{36}\epsilon^2\right) \end{aligned} \tag{16}$$

With

$$A_2 = \frac{9Gmr^2}{8\pi^2 f_{2rotor}^2 d^4} \tag{17}$$

And at four times the rotation frequency (f_{4rotor}) the amplitude is

$$\begin{aligned} a(f_{4rotor}) &= \frac{2C_4Gm}{4\pi^2 f_{4rotor}^2 d^2} \\ &= \frac{175Gmr^4}{128\pi^2 f_{4rotor}^2 d^6} \\ &= A_2\frac{175}{144}\epsilon^2 \end{aligned} \tag{18}$$

2.2 Impact of a vertical offset

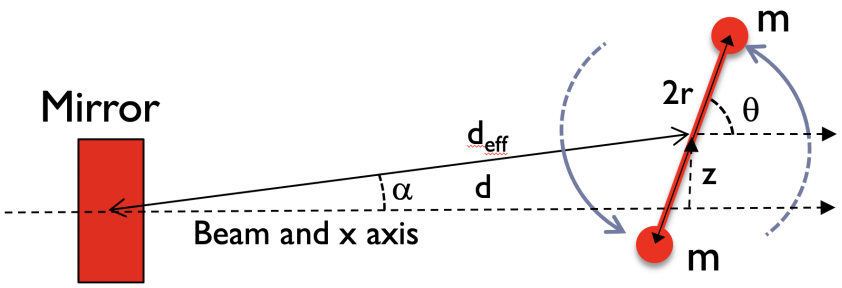

Figure 3: Case with a vertical offset for the rotor

The rotor (assumed to rotate in the vertical plan) could be slightly off by a distance z from the interferometer plane. Then, the effective distance (d_{eff}) between the mirror and rotor centers (see figure 3) is slightly larger:

$$d_{eff} = d\sqrt{1+(z/d)^2} \tag{19}$$

The projection of the force on the interferometer plan is also reduced by a factor:

$$R = \frac{d}{d_{eff}} = \frac{1}{\sqrt{1+(z/d)^2}} \tag{20}$$

Therefore, the overall effect on the mirror displacement due to a z offset is a reduction of the displacement by a factor $(1+(z/d)^2)^{5/2}$. This computation assumed that the mirror is point-like.

The phase of the signal will also be impacted by a factor $\sqrt{1+(z/d)^2}$.

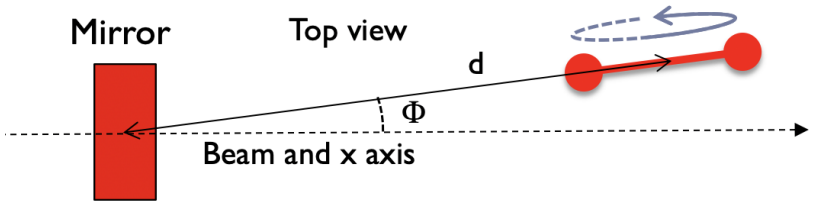

Figure 4: Case with angular offset in the interferometer plan (top view)

2.3 Impact of the rotor not along the beam axis

Usually, the rotor (still in the plan of the interferometer) is not along the beam axis, but installed with an angle Φ relative to the beam axis (see figure 4). If d is again the distance between the mirror and rotor centers, then the force applied to the mirror is the same as in the previous section. But the displacement along the x axis is reduce by a factor $cos\Phi$. Since it is a geometrical factor, it is the same factor for all harmonics.

The phase of the signal is unchanged since the rotor is turning in the vertical plan.

2.4 Extended rotor; signal at twice the rotor frequency

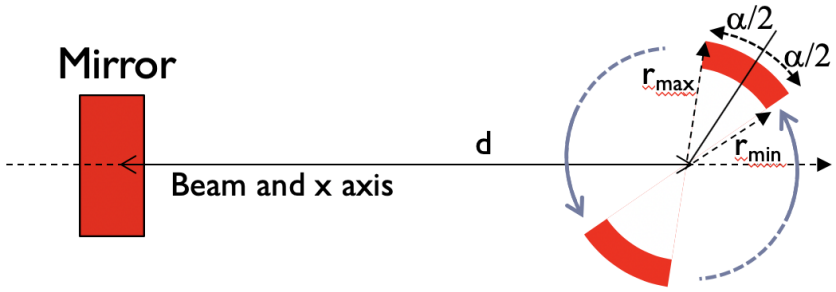

Figure 5: Rotor made of two sectors

Real rotors are not point-like masses. One simple geometry is to consider two sectors of thickness b, with an opening angle α (from 0 to π) and inner and outer radii r_{min} and r_{max} like in figure 5. To compute the expected signal, we consider that the rotor is the sum of the small sectors of opening angle $\delta\phi$, radius δr and thickness δb. The mass of this small sector is $\rho r\delta\phi\delta r\delta b$, with ρ being the density of the rotating mass. Then the expected signal amplitude for this small rotor part is:

$$\delta a(f_{2rotor}) = \frac{9G\rho r^3\delta\phi\delta r\delta b}{8\pi^2 d^4 f_{2rotor}^2}\left(1+\frac{25}{36}\epsilon^2\right) \tag{21}$$

When integrating over r and b, the signal adds up linearly. But when integrating over ϕ, the sum is not anymore coherent. Starting from the center of the sector, a factor $\cos 2\phi$ must be included. The angular integral is therefore:

$$\int_{-\alpha/2}^{\alpha/2} \cos 2\phi\delta\phi = \sin(\alpha) \tag{22}$$

Therefore the overall amplitude is:

$$a(f_{2rotor}) = \frac{9G\rho b}{8\pi^2 d^4 f_{2rotor}^2}\sin(\alpha)\left[\frac{1}{4}(r_{max}^4 - r_{min}^4) + \frac{25}{216d^2}(r_{max}^6 - r_{min}^6)\right] \tag{23}$$

which could be written as:

$$a(f_{2rotor}) = \frac{K}{d^4 f_{2rotor}^2} C_{rotor} \tag{24}$$

with

$$K = \frac{9G\rho b}{8\pi^2 f_{2rotor}^2} \sin(\alpha) \left[\frac{1}{4} (r_{max}^4 - r_{min}^4) \right] \tag{25}$$

and

$$C_{rotor} = 1 + \frac{25}{54d^2} \frac{(r_{max}^6 - r_{min}^6)}{(r_{max}^4 - r_{min}^4)} \approx 1 + \frac{25}{54} \left(\frac{r_{max}}{d} \right)^2 \tag{26}$$

The maximum coupling factor is achieved with $\alpha = \pi/2$, i.e. when the rotor is divided in four sectors of the same volume, alternating empty and full volumes. In this case, any error on the opening angle of the rotor cancels at first order. The coupling factor depends only on the rotor thickness and radii, mostly its outer radius.

2.5 Extended rotor; signal at four times the rotor frequency

When integrating of ϕ, from the center of the sector, a factor $\cos(4\phi)$ must be included. The integral is therefore:

$$\int_{-\alpha/2}^{\alpha/2} \cos(4\phi) d\phi = \frac{1}{2} \sin(2\alpha) \tag{27}$$

The maximum coupling factor is achieved with $\alpha = \pi/4$. In this case, the optimal configuration is to divide the rotor in height sectors of the same volume, alternating empty and full volumes. If $\alpha = \pi/2$, then the signal at four times the rotor frequency disappear.

2.6 Extended mirror

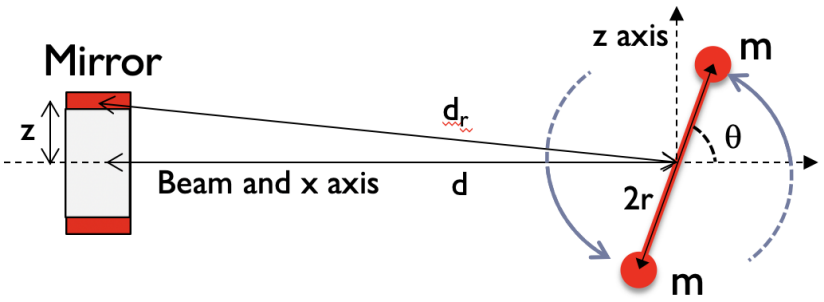

Figure 6: Mirror as a set of rings

The mirror has a finite diameter that can not be neglected. The mirror can be seen as the sum of small rings of diameter z, see figure 6. For a given ring, the distance to the rotor, d_r is slightly larger by a factor:

$$d_r/d = \sqrt{1 + (z/d)^2} \tag{28}$$

Therefore, the force and mirror displacement is reduced by the fourth power of this factor (taking only the leading term). Since the mass of the ring goes as the ring diameter, the average

correction factor to be added as an extra factor in equation 24 is :

$$\begin{aligned} C_{mirror} &= \frac{\int_0^{r_{mirror}} (1+(z/d)^2)^{-2} z dz}{\int_0^{r_{mirror}} z dz} \\ &\approx \frac{\int_0^{r_{mirror}} (1-2(z/d)^2) z dz}{\int_0^{r_{mirror}} z dz} \\ &= 1 - \frac{2}{d^2} \frac{\int_0^{r_{mirror}} z^3 dz}{\int_0^{r_{mirror}} z dz} \\ &= 1 - \left(\frac{r_{mirror}}{d}\right)^2 \end{aligned} \tag{29}$$

The corrections due to the mirror thickness (thin disks along x) are smaller. Unlike for the radial effect that always lead to a larger distance between a mirror ring and the rotor, the distance between a close or a far part of the mirror could be smaller or larger than the average distance. Therefore, this effect cancel out when doing the computation at first order.

3 Parameters of the NCal-200

The NCal-200 have been designed and built at LAPP in 2018. Figure 7 shows the drawings of the NCal-200 rotor. Using the definitions of the previous section, the nominal rotor parameters are:

- Thickness: $b = 0.074$ m
- Opening angle: $\alpha = \pi/2$
- Inner radius:$r_{\min} = 0.032$ m
- Outer radius: $r_{\max} = 0.095$ m
- Density $\rho = 2805$ kg/m^3 (expected density for aluminium 7075)

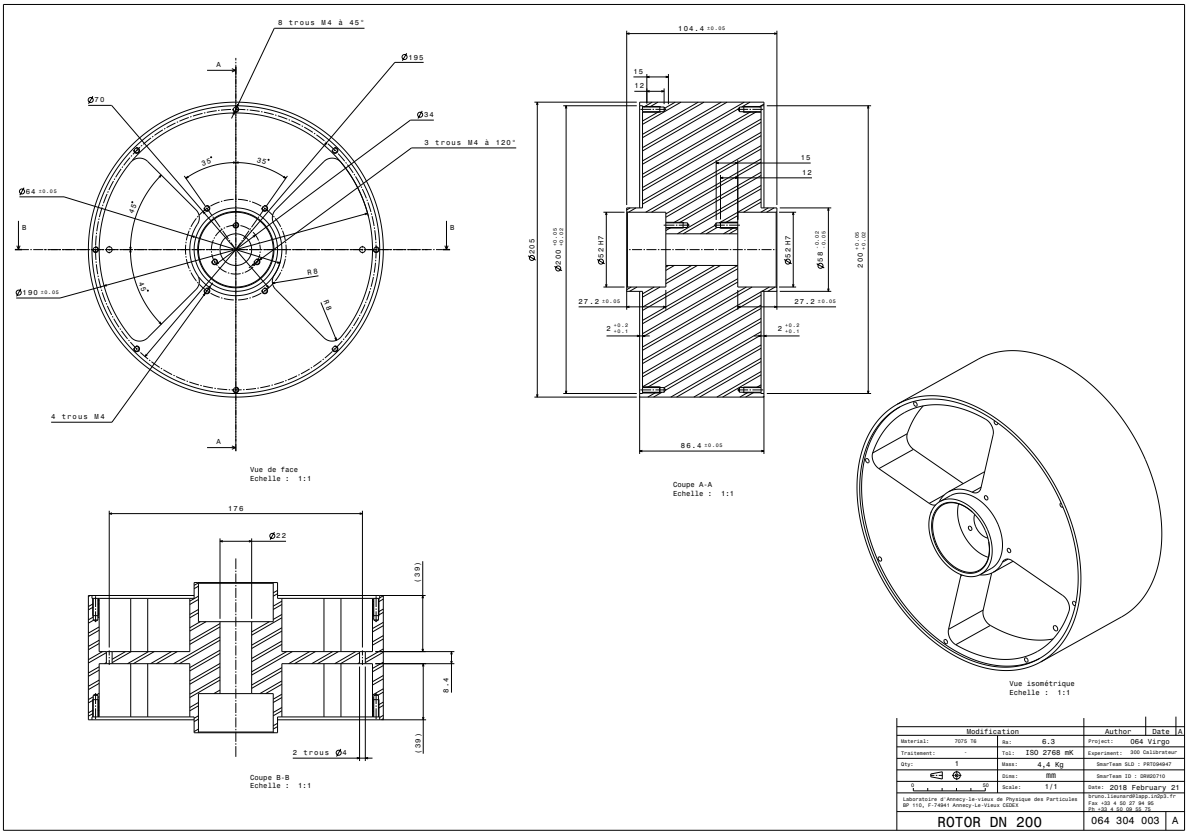

Figure 7: Drawing of the NCal200 rotor

The rotor has been measured on November 14, 2018 by the "Initial" company, located near Annecy. The deviations to the nominal values of the drawing are presented in figure 8. The critical parameters are:

- The thickness of the rotor: a systematic deviation of about 0.1 mm is observed on both sides (see the points on the blue part). Therefore, when computing the expected displacement, the b parameter will be reduced by 0.2 mm: $b = 0.0738$. The uncertainty on b will be this correction.
- The inner diameter (at $r_{\max} = 95$ mm) is larger by 0.045 mm on average. Again, when doing computations, we will correct for this change and take $r_{\max} = 0.095045$ m. The uncertainty on $r_{\max}$ will be this correction.

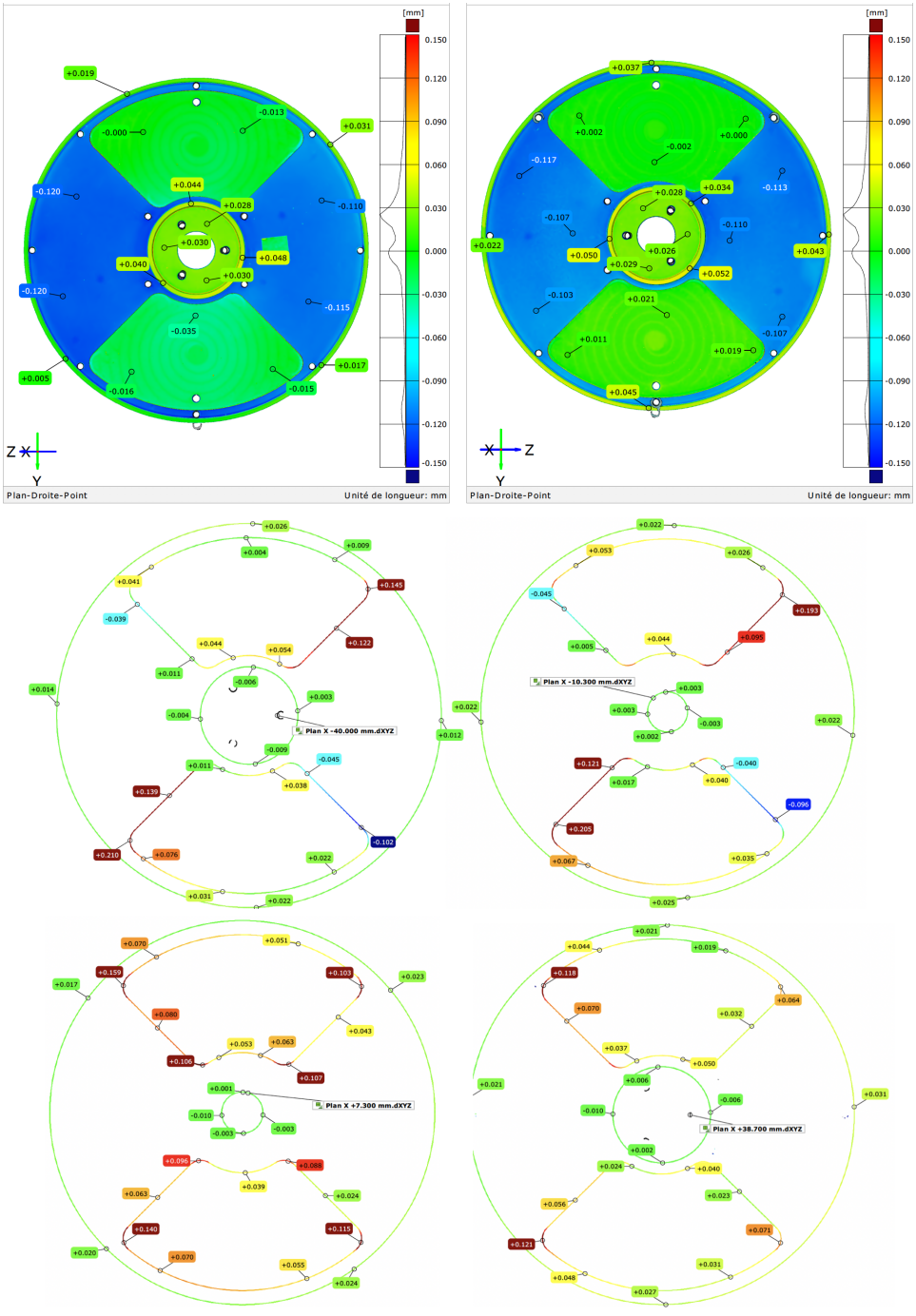

Figure 8: Measurements of the surface defects; the two top plots are for both sides of the rotor, the four bottom plots are for radial measurement made on different plans, located at -40 mm, -10 mm, + 7.3 mm and +38.7mm of the average plan. All values are in mm relative to the reference values of the drawings (see figure 7).

The NCal rotation frequency is monitored by a photodiode system monitoring light pulses when a hole in the rotor is in front of a LED. The photodiode electronic and DAQ readout introduce some delay. This delay is known by shining on the readout photodiode the light of a LED powered by the timing system and looking closely at the time of arrival of the pulse generated every new second (the 1 PPS signal). Figure 9 is showing this test. We can see that the transition starts after almost one full sample of 50 μs (the signal is sampled at 20 kHz), after the change of second. Therefore, the raw observed delay is around 45 μs. Since this is done on the north end building, the 1 PPS of the timing system is delivered with a 16 μs delay. Therefore, the effective delay is 61 μs. The uncertainty on this number might be as large as 50μs. This uncertainty could be reduced in the future by additional measurement with the data collected at a higher sampling rate.

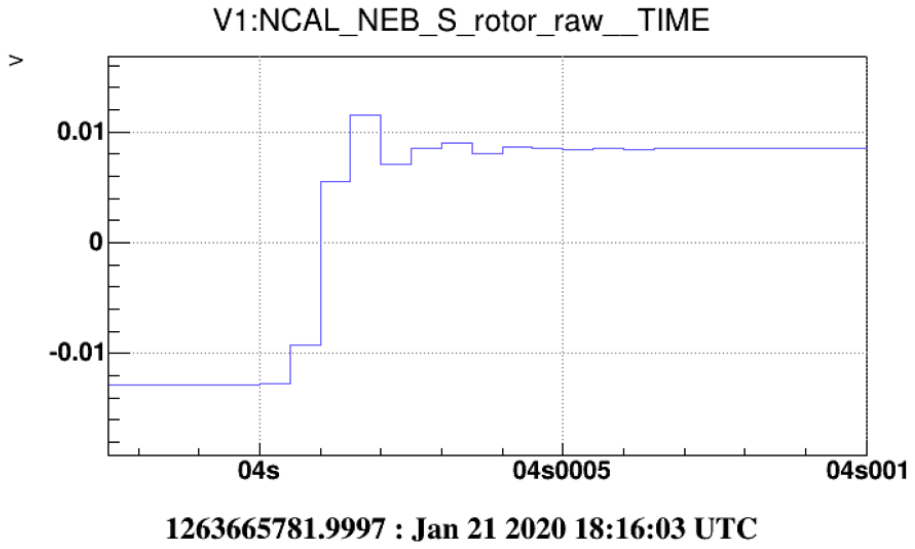

Figure 9: Zoom on the 1 PPS test signal used to measure the photodiode delay).

4 Reconstructing the $h(t)$ NCal signal

4.1 Getting the NCal information

The current NCal motor is a standalone system and therefore the NCal rotation is independent of the Virgo timing system. The phase and rotation speed is not known a priori, but need to be extracted from the data, using the optical pulses of the "V1:NCAL_NEB_N_rotor_raw" channel, see Fig. 10.

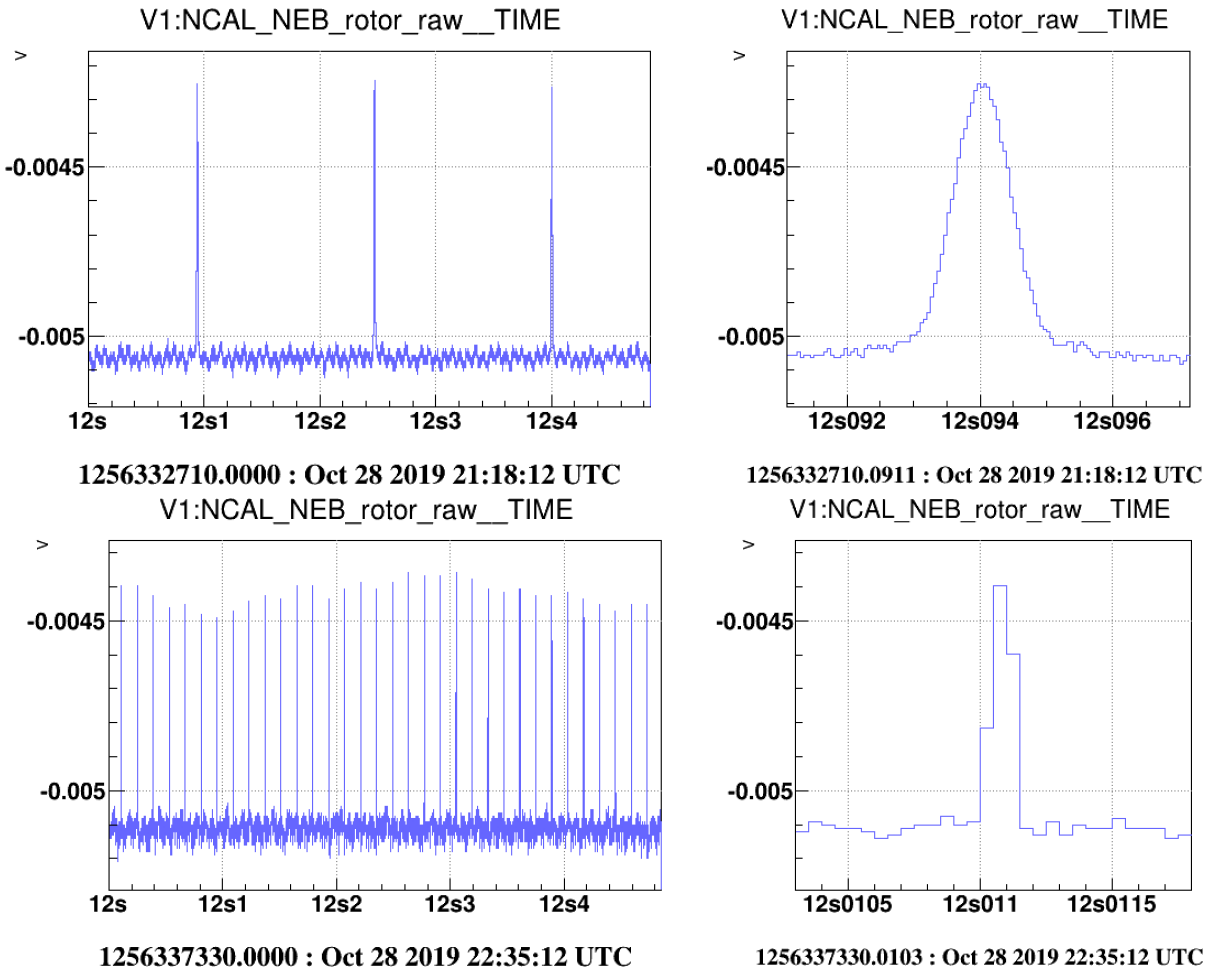

Figure 10: Monitoring of the rotor rotation for two frequencies: 6.7 Hz (top) and 71 Hz (bottom). The right plots are just zoom around one pulse.

The time of each individual pulses is computed by taking the average value of the time of the rising and falling fronts. Each of these times is computed by doing a linear interpolation of the time of the samples around the crossing of 50 % of the pulse height, going up or down. This method should give the central value of the pulse and being independent of the rotor speed.

Once the pulse times are known, the rotation period is just the time difference between two pulses and the instantaneous frequency the invert of this period.

4.2 Extracting the NCal amplitude from the $h(t)$ spectrum

The NCal amplitude is extracted by doing the transfer function between the $h(t)$ channel and a signal monitoring the NCal rotation. For this purpose, a set of pure sine-waves of unit amplitude is built with the same sampling rate as the $h(t)$ channel. Their frequencies are N times the rotor frequency (typical value: N=2). The NCal $h(t)$ amplitude for the harmonic N of the rotor is then computed by reading, at the harmonic frequency, the transfer function value between the

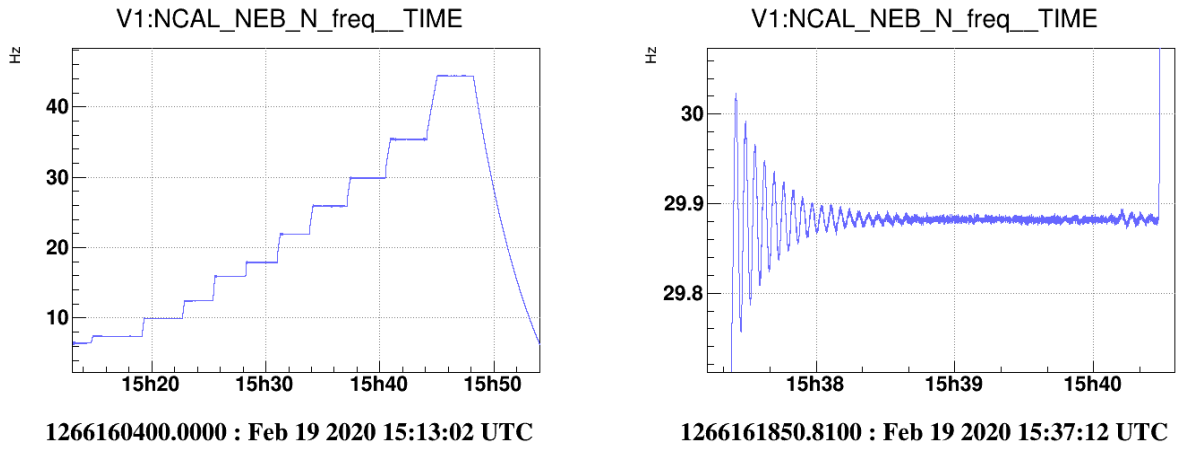

Figure 11: Reconstructed rotor frequency as function of time. The right plot is a zoom of one step of the scan. Once the requested rotation speed is reached, the frequency stabilizes within less than a minute.

reconstructed $h(t)$ and the corresponding sine wave. This transfer function is computed over several seconds (20 seconds for the Feb. 19 data), meaning that a new value of the NCal h(t) recovered amplitude is available with the same period.

The phase is extracted in the same way. Given the position of the hole in the rotor as well as the LED/photodiode position, when the two massive sectors are vertical, the phase is zero.

4.3 Checking the procedure to compute the NCal amplitude

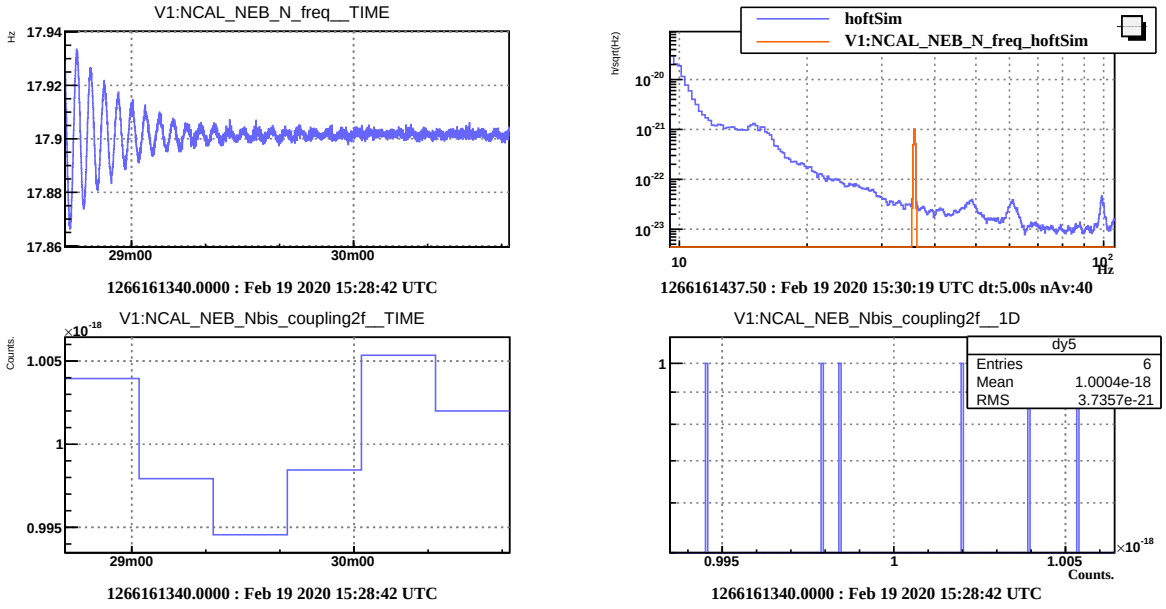

Figure 12: Check of the NCal amplitude measurement. See text for comments

In order to check the validity of the extraction method of the NCal amplitude from the h(t) stream, a fully simulated h(t) stream was built and then processed using the regular processing code. This simulated stream was first built by making a fake h(t) channel using the FdIO library with the "FDIN_ADD_SURROGATE_CHANNEL" configuration key. The reference spectrum was extracted from 20 seconds of real h(t) data starting from GPS = 1266160240, i.e., just

before the NCal injections of February 19. Then, a pure sine wave was added with a frequency extracted from the NCal_N, with an amplitude set to $10^{-18} f^{-2}$.

The top left plot of figure 12 shows the instantaneous frequency for the 120 seconds of test. The top right plot presents the simulated noise, plus the injected amplitude (red trace). The bottom plots shows the recovered amplitude times the frequency squared as function of time (left) and as histogram (right). The recovered amplitude relative to the injected one is $1.0004 \pm 1.5 \times 10^{-3}$, in good agreement with the expected value of 1.

5 Expected NCal signal

5.1 Expected positions of the two NCal

As explained in the introduction, two NCal-200 have been installed on the south side of the north end tower (see figure 13). The position "4-5" on the NCal support beam has been surveyed relatively to the mirror nominal position, see logbook entry # 45131 (`https://logbook.virgo-gw.eu/virgo/?r=45131`:

- $x = 0.8139 - 0.0129 = 0.801$ m
- $y = 4.6314 - 5.7877 = -1.1563$ m (y is along the beam axis)

Therefore the position "4-5" is at a distance $d = 1.4066$ m from the mirror and make an angle $\Phi = 0.6058$ rad relative to the beam axis. Since the NCal close to the mirror (with data named NCal_N) is offset by 140 mm, its distance to the mirror is $d = 1.4066 - 0.14 = 1.2666$ m. The other NCal far to the mirror (with data named NCal_S) is offset by 680 mm (400 + 2x140 mm), its distance to the mirror is $d = 1.4066 + 0.4 + 0.14 = 1.9466$ m.

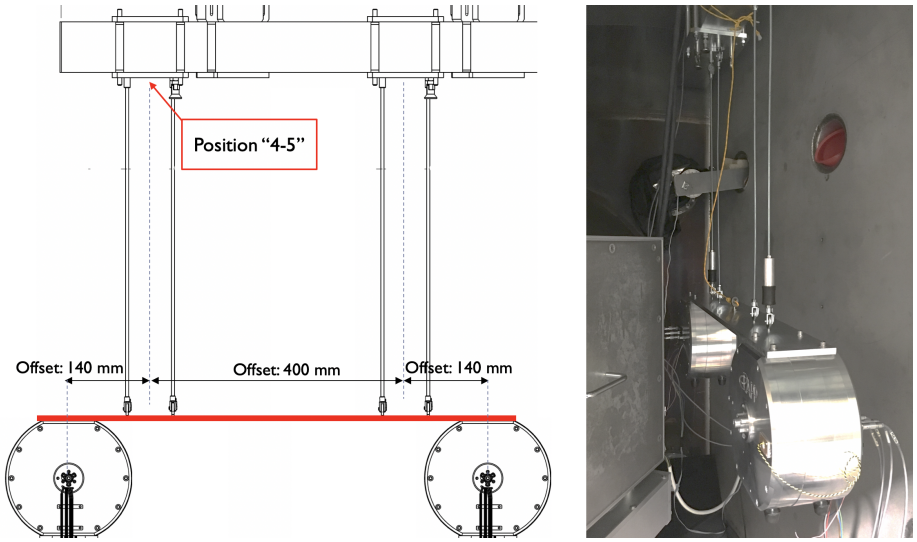

Figure 13: Layout of the two NCal-200 suspended on the south side of north end tower.

5.2 Expected NCal calibration line amplitude

Using equations 24, 29, the NCal parameters and the interferometer arm length of 3000 m, we can write the observed $h_N(t)$ amplitude of the near NCal (NCAL_N data) at a given distance as:

$$h_N(f_{2rotor}) = 3.32 \times 10^{-18} f_{2rotor}^{-2} \tag{30}$$

For the far NCal (NCAL_S data), the $h_S(t)$ amplitude is

$$h_S(f_{2rotor}) = 6.01 \times 10^{-19} f_{2rotor}^{-2} \tag{31}$$

6 Analysis of the February 19, 2020 data

6.1 NCal signal in the h(t) data

NCal data have been collected on February 19, 2020. A frequency scan was performed with the near NCal, stopping at eleven frequencies for few minutes each time. The far NCal was set to run at a constant frequency, leading to an $h(t)$ signal at 35 Hz. Figure 14) present a time-frequency plot of the h(t) channel during this test. The only visible traces are the two NCal signals. There is no indication of unexpected coupling between the NCal and the interferometer (through, for instance, direct mechanical coupling) that would be seen as signal at the rotor frequency (half frequency of the NCal signal) or higher harmonics.

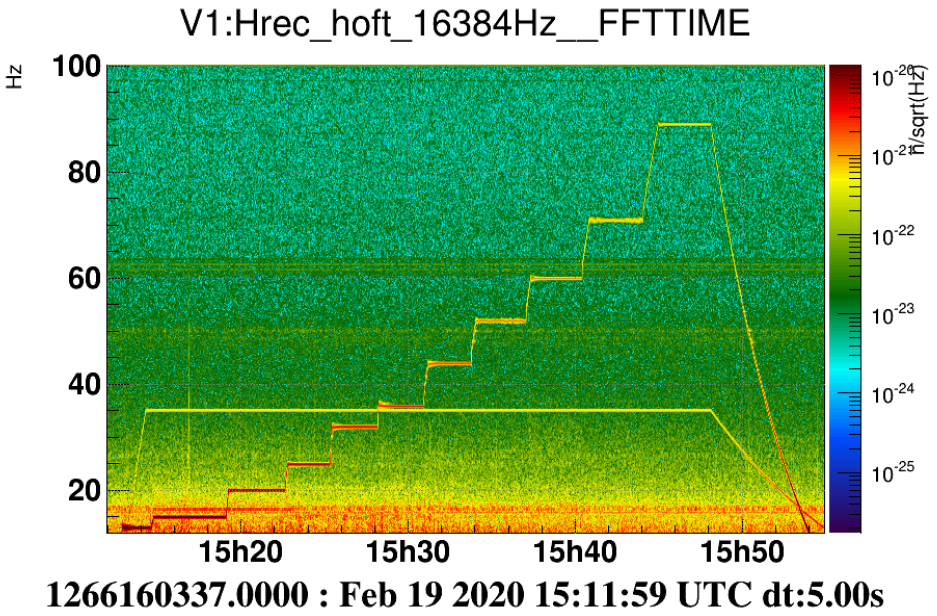

Figure 14: $h(t)$ time frequency plot during NCal lines injection

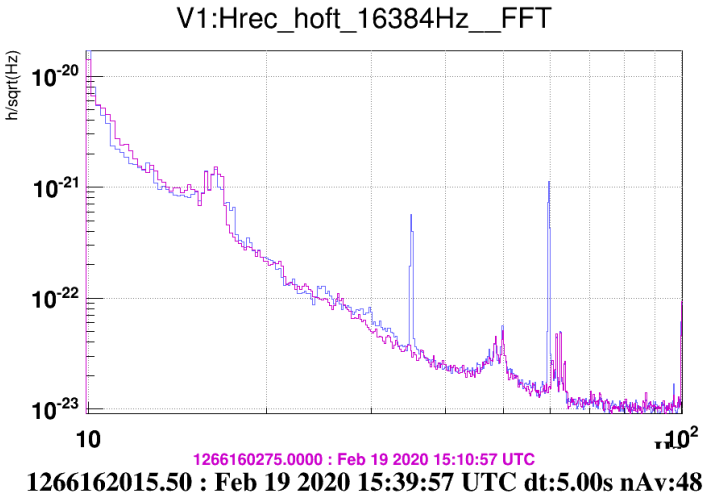

Figure 15: Spectrum where the two NCal lines are well visible (blue curve) at 35 and 60 Hz, compared to a reference spectrum (pink curve) taken just before the start of the NCal operation

Figure 15 is comparing the h(t) spectrum before and after the start of the two NCal. Again, the only change in the spectrum is the two NCal lines.

6.2 NCal checks versus frequency

Using reconstructed data from February 19 2020, we can build the plots of figure 16 that presents the comparison between the injected signal and the recovered one. This is also compared to the same same check made with the coils injections. While the shapes are roughly similar, there is a significant offset of 3 to 5 % for the recovered NCal calibration line amplitude. The plotted error bars are just statistical. The systematic errors will be discussed in a following section.

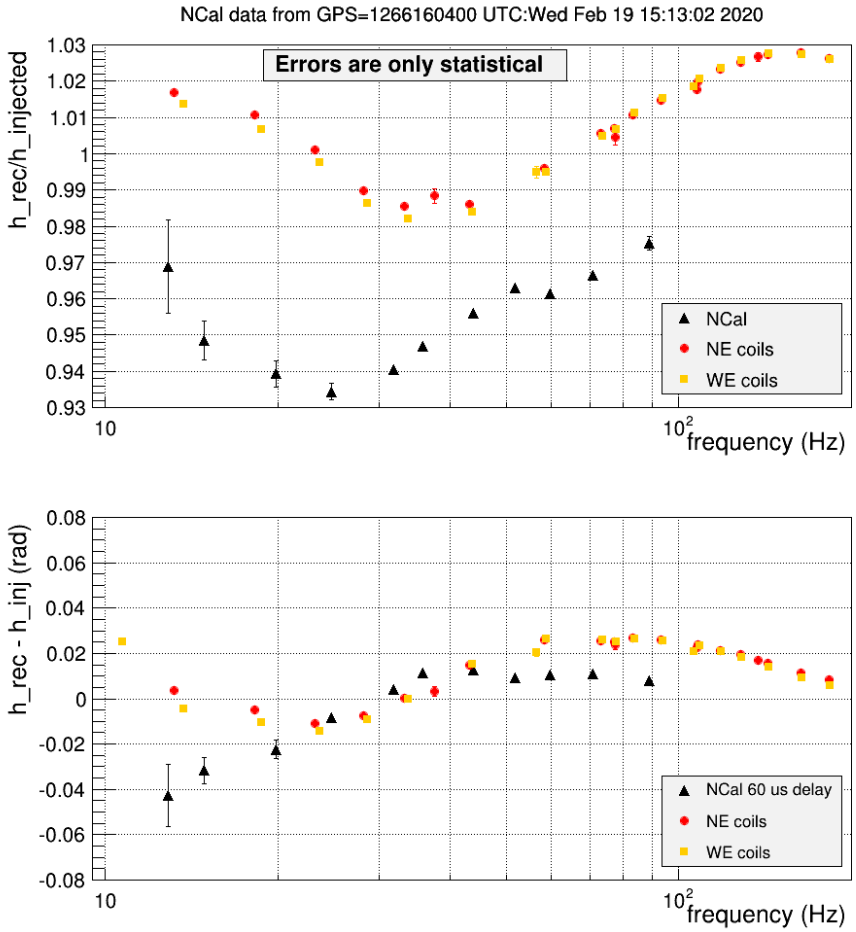

Figure 16: Top plot: ratio between the expected (or injected) and the recovered h(t) signal. Bottom plot: phase difference between the expected and recovered h(t) signal. Data from February 19, 2020. The error bars are just statistical.

6.3 Checking the mirror-NCal distance using the NCal signals

The two NCal have been placed at a well know relative distance $s = 680$ mm (with an error less than 0.5 mm) in order to determine the absolute mirror to the first NCal distance d_0.

From equations 24 and 29, we can write the observed amplitude at a given distance as:

$$h(d) = \frac{K}{d^4 f^2 L} C_{rotor}(d) C_{mirror}(d) \tag{32}$$

where $C_{rotor}(d)$ and $C_{mirror}(d)$ are close to 1 and slowly changing with the distance d, and L the interferometer arm length.

Therefore, it is convenient to define

$$\begin{aligned} H(d) &= h(d) f^2 \\ B(d) &= \frac{H(d)}{C_{rotor}(d) C_{mirror}(d)} \end{aligned} \tag{33}$$

These two quantities are frequency independent (at first order). Data have been collected with the two NCal rotating at almost the same frequency (to avoid calibration frequency-dependent effects). The observed amplitudes (see figure 6.3) and correction factors computed with the nominal distances are:

distance	$H(d)$	$C_{rotor}(d)$	$C_{mirror}(d)$	$B(d)$
d_0	$3.146 \times 10^{-18} \pm 4.9 \times 10^{-21}$	1.0026	0.9809	$3.199 \times 10^{-18} \pm 4.9 \times 10^{-21}$
$d_0 + s$	$5.6516 \times 10^{-19} \pm 1.3 \times 10^{-21}$	1.0011	0.9919	$5.6913 \times 10^{-19} \pm 1.3 \times 10^{-21}$

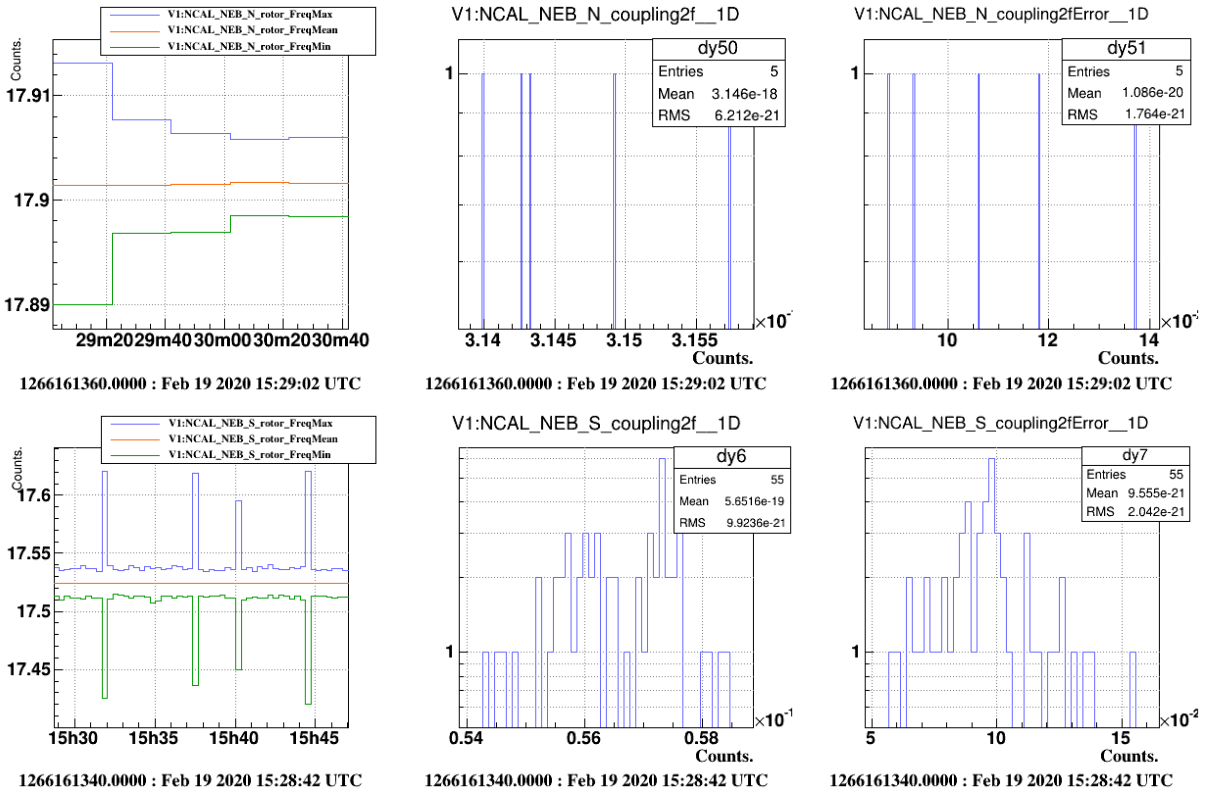

Figure 17: Data used to measure the NCal to mirror distance. The top set of plots is for the NCal near the mirror (located at d_0,) the bottom set for the NCal far from the mirror. Both NCal were rotating at almost 18 Hz. The "coupling2f" parameters are the $H(d)$ parameter of equation 33, in other words, the h(t) amplitude at twice the rotor frequency multiplied by the squared of the observed frequency.

Assuming that the two NCal are identical, we can derive the following equation:

$$\frac{B(d_0)}{B(d_0+s)} = \frac{(d_0+s)^4}{d_0^4} \tag{34}$$

and therefore

$$d_0 = s\Big[\Big(\frac{B(d_0)}{B(d_0+s)}\Big)^{1/4} - 1\Big]^{-1} \tag{35}$$

Using this, we get the following result:

$$d_0 = 1.2599 \pm 0.0025 \text{ m} \tag{36}$$

meaning an offset of 6.7 ± 2.5 mm compared to the geometrical position, where the uncertainty is just coming from the statistical errors of the NCal signal in the h(t) spectrum. As explained,

this measurement assumed that the two Ncal are identical. To set the scale, a 0.1 % difference of the rotor coupling factor K (see equation 24) translate to a 0.9 mm offset. The differences between the two NCal could be searched by taking additional measurements (during the end of run measurements) where the two NCal are swapped.

We have seen that there is an offset between the injected and recovered lines for the near NCal. Using the expected coupling factor (see section 5.2) and the above table, we have the following ratio at $f_{\text{rotor}} \approx 18Hz$:

- h_rec/h_inj = 0.9474 ± 0.0016 for the near NCal (NCal_N)
- h_rec/h_inj = 0.9404 ± 0.0023 for the far NCal (NCal_S)

One can see that this "low" recovered amplitude is even larger for the far NCal. This means that the observed deficit for the near NCal could not be solved by a better knowledge of the NCal position.

7 Systematic uncertainties and discussion

The following table summarizes the main sources of uncertainties and their impact on the expected injected calibration line.

The first three lines of the table capture the uncertainties on the NCal position. The leading one is the mirror to NCal distance that is difficult to directly measure. The values quoted here is derived from the measured offset (see section 6.3).

The next three lines are reporting the possible NCal geometrical defects. A global test was made by measuring the weight of the rotor: 4.837 kg, and comparing it to the expected CAD value: 4.845 kg for the nominal parameters. This is just a 8 g difference, that actually correspond to the reduction of 200 μm of the rotor thickness discussed in section 3: $\pi\ 0.0002 \times 0.095^2 \times 2805/2 = 8$ g. This agreement is an indication that the uncertainties on the rotor parameter are correct.

The model error is rather arbitrary and has been taken as 2% a value a bit larger than the correction to convert a point like model to the extend rotor/mirror.

Parameter			Relative impact	
name	value	uncertainty	formula	value (%)
distance (m) d	1.26	0.007	$4\delta d/d$	2.3
angle Φ (rad)	0.606	0.004	$\delta\Phi \sin\Phi$	0.23
vertical position z (m)	0	0.02	$5/2(z/d)^2)$.	0.06
density ρ (SI)	2805	5	$\delta\rho/\rho$	0.18
thickness b (mm)	74	0.2	$\delta b/b$	0.27
$r_{\max}$ (mm)	95	0.1	$4\delta r_{\max}/r_{\max}$	0.42
model			guess	2
Total			quadratic sum	3.1

The overall systematic uncertainty is around 3%. This is a bit smaller than the discrepancy observed between the between the NCal and the coil or PCal calibration, although it is not fully incompatible given the 1 to 2 % absolute systematical uncertainty on the coil calibration.

One of the more sensitive parameters is the mirror to NCal distance. Its estimated error is half of the observed discrepancy between the NCal and the coil or PCal calibration. However, the measured distance is smaller than the nominal one, which would lead to a larger discrepancy. This means that the observed discrepancy is probably not coming from the mirror to NCal distance.

In any case, the NCal is a too new technic to conclude that there is an issue with the Virgo calibration. It is much more likely that some parameters of the NCal are not the expected ones, or the model is incomplete, or the calibration lines are not correctly extracted, or... Further studies are needed to understand this disagreement.